Electronic Supplementary Material (ESI) for Chemical Science.

Supporting information

Investigating the role of the strong field ligands in [FeFe] hydrogenase: Spectroscopic and functional characterization of a semi-synthetic mono-cyanide active site

Marco Lorenzi,[a, †] Joe Gellett,[b, †] Afridi Zamader,[a,c] Moritz Senger,[d] Zehui Duan,[b] Patricia Rodríguez-Maciá[b,*] and Gustav Berggren[a,*]

a. Department of Chemistry – Ångström Laboratory, Molecular Biomimetics, Uppsala University, 75120 Uppsala, Sweden.

email: Gustav.berggren@kemi.uu.se

b. Department of Chemistry, University of Oxford, Inorganic Chemistry Laboratory, South Parks Road, OX1 3QR, United-Kingdom.

c. Laboratoire de Chimie et Biologie des Metaux, iRTSV-LCBM/Biocat, UMR 5249 Commissariat à l'Energie Atomique (CEA) Grenoble, 17, rue des Martyrs, 38054 Grenoble Cedex 09, France

d. Department of Chemistry – Ångström Laboratory, Physical Chemistry, Uppsala University, 75120 Uppsala, Sweden.

Table of contents

Experimental details

Expression, purification and artificial maturation

$[(\mu\text{-adt})Fe_2(CO)_4(CN)_2]^{2-}$ (adt = azadithiolate, $^-SCH_2NHCH_2S^-$) (complex **1**) and $[(\mu\text{-adt})Fe_2(CO)_5(CN)]^-$ (complex **2**) were synthesized following published procedures.[1, 2]

Chlamydomonas reinhardtii HydA1 (HydA1) was expressed, purified and reconstituted as previously reported, with minor modifications.[3] In short, a BL21(DE3) *E.coli* strain was transformed with a codon-optimized sequence for *HydA1* on a pET11a plasmid. After expression, the protein was purified using a StrepTrap® column mounted on an Äkta-Ready® FPLC system (Cytiva). After semi-enzymatic [4Fe4S] cluster reconstitution, yielding the so-called *apo-* form of the enzyme (*apo-HydA1*, containing the [4Fe-4S] cluster but lacking the binuclear site) the enzyme was artificially matured using **1** or **2**, under a pure Ar atmosphere (MBRAUN, DE). For complex **1**, 100 - 150µM reconstituted HydA1 were mixed with 6x molar excess of **1** and 2 mM sodium dithionite in a 100 mM Tris/HCl pH 8, 200 mM KCl buffer (yielding **1**-HydA1). The mixture was incubated for 90 minutes at room temperature and the reaction mix was then cleaned using a PD10 desalting column, pre-equilibrated with a 100 mM Tris/HCl pH 8, 200 mM KCl buffer. For complex **2**, 100 - 150 µM reconstituted HydA1 were mixed with 5x molar excess of **2** and 10 mM sodium dithionite in a 25 mM Tris/HCl pH 8, 25 mM KCl, 10% acetonitrile buffer (yielding **2**-HydA1). The mixture was incubated for 90 minutes at room temperature and the reaction mix was then cleaned via repeated buffer exchange using 30 kDa-cutoff centricon tubes and a 25 mM Tris/HCl pH 8, 25 mM KCl, 10% acetonitrile buffer. Samples used for FTIR studies underwent a further buffer exchange step using a 10 mM Tris/HCl pH 8 buffer. Mutants were obtained using a modified version of the QuickChange PCR protocol, then expressed and purified as outlined above.

Desulfovibrio desulfuricans HydAB (HydAB) was expressed, purified and reconstituted as described previously.[4] Briefly, HydAB was produced recombinantly in *E. coli* BL21 (DE3) ΔiscR cells as a fusion protein with a C-terminus Strep-II tag on the large subunit. Cells were grown aerobically, and made anaerobic before induction. Cells were harvested anaerobically in a N_2 glovebox (Glove Box Technology Limited, UK), and cell lysis was performed anaerobically by sonication. The protein was purified using Strep-tag affinity chromatography. Artificial maturation was carried in 100 mM Tris/HCl + 150 mM NaCl pH 8 under strict anaerobic conditions inside a N_2 glovebox (Glove Box Technology Limited, UK), by reconstituting 100 µM of apo-HydAB either with 5x excess of complex **1** (yielding **1**-HydAB) or with 5x excess of complex **2** (yielding **2**-HydAB). In both cases, the maturation mixture was left to react for 48 h at 35 °C, and the excess of the synthetic mimic was removed on a PD-10 desalting column. **1**-HydAB was shaken at 15 °C for 48 h in the dark to allow CO release, while **2**-HydAB was concentrated directly after removing the excess of synthetic mimic. The samples were concentrated on 30 kDa MWCO concentrators, and frozen at -80 °C until use.

Activity assays

H_2-evolution assays were performed under an oxygen-free argon atmosphere. Aliquots of the maturated enzymes were transferred in 100 mM phosphate buffer pH 6.8 containing 10 mM methyl viologen, in rubber-sealed glass vials. The reaction was then initiated by the rapid addition of sodium dithionite (NaDT, final conc. 100 mM) and the vials were incubated at 37°C for 15 min. The amount of H_2 produced in the unit of time was then determined by sampling the headspace atmosphere and running the samples on a PerkinElmer Clarus 500 gas chromatograph (GC) equipped with a thermal conductivity detector (TCD) and a stainless-steel column packed with Molecular Sieve (60/80 mesh). The operational temperatures of the injection port, the oven and the detector were 100 °C, 80 °C and 100 °C, respectively. Argon was used as carrier gas at a flow rate of 35 mL min^{-1}.

Similarly as described previously,[4] H_2 uptake solution assays for HydAB were performed by colorimetric analysis by following the reduction of 1 mM benzyl viologen (Sigma Aldrich), at 600 nm (ε_{600} = 7.0 $mM^{-1}\,cm^{-1}$), by the enzyme in a 50 mM Tris/HCl pH 8 buffer saturated with H_2 gas at 25°C. Assays were performed in 1.5 mL plastic cuvettes inside a N_2 glovebox (Glove Box Technology Limited, UK) using a Cary 60 UV-Vis spectrophotometer with a cell holder (Agilent) and a Peltier accessory for temperature control. **1**-HydAB served as a positive control, and showed a specific activity for H_2 oxidation of 45900 ± 7400 µmol H_2 $mg_{protein}^{-1}$ min^{-1}.

FTIR Spectroscopy

2 µL of a **2-**HydA1 (or **2**-HydA1^{A94S}) solution (0.3 - 0.6 mM) in 10 mM Tris buffer (pH 8) was deposited on the ATR crystal in an anaerobic Glovebox (Mbraun). The ATR unit (BioRadII, Harrick) was then sealed with a custom build PEEK cell that allows for gas exchange and illumination (analogous to the system used in refs.[5, 6]). Spectra were recorded on a Vertex V70v FTIR spectrometer (Bruker). Sample´s hydration was controlled using dry 100% nitrogen gas and buffered (10 mM Tris/HCl, pH 8) aerosol, as previously described.[7] Light treatment was applied using a Schott KL2500LCD cold light source. Air exposure was obtained opening the ATR unit to the atmosphere. Spectra were recorded with 2 cm^{-1} resolution, a scanner velocity of 80 Hz and represent the average of 100 - 1000 scans each. All experiments were performed at room temperature and 1 atm pressure.

For **1**-HydAB and **2**-HydAB, FTIR spectra were measured in a commercial IR transmission cell (PIKE) on 5 µL of ≈ 1 mM samples (20 mM Tris/HCl + 30 mM NaCl, pH 8) deposited between two CaF_2 windows (31.8 mm x 1.5 mm, Crystan) separated with a 25 µm Teflon spacer (PIKE Technologies) coated with vacuum grease and closed. Spectra were measured at room temperature inside an anaerobic dry glovebox (Glove Box Technology Ltd. UK, <2 ppm of O_2, <85 °C dew point) on a Bruker Vertex 80v FTIR spectrometer equipped with a nitrogen cooled Bruker mercury cadmium telluride (MCT) detector. Spectra were collected in the double-sided, forward-backward mode with a resolution of 2 cm^{-1}, an aperture setting of 0.5 mm and a scan velocity of 20 kHz. Spectra were recorded using OPUS software and are the average of 1024 scans. Data were processed using home-written routines in the MATLAB and OPUS. All the figures are prepared in Origin.

EPR Spectroscopy and simulations

EPR samples were prepared with 150 – 200 µL of a 150 µM enzyme solution in 25 mM Tris/HCl pH 8, 25 mM KCl and 10% acetonitrile buffer. The EPR tubes were sealed anaerobically and flash frozen in liquid nitrogen. Measurements were performed on a ELEXYS E500 spectrometer (Bruker) using an ER049X SuperX microwave bridge in a SHQ0601 cavity (Bruker) equipped with a continuous flow cryostat and using an ITC 503 temperature controller (Oxford Instruments). Cryogenic temperatures were achieved using liquid helium as a coolant. The spectrometer was controlled by the Xepr software package (Bruker). Spectra were processed using homemade routines in MATLAB (Mathworks) and simulations were performed using the pepper function from the MATLAB Easyspin package[8].

Protein film electrochemistry

For **1**-HydA1 and **2**-HydA1, protein film electrochemistry experiments were carried out with a gas-tight, water-jacketed three-electrode electrochemical cell contained inside an anaerobic Ar filled glovebox (MBraun, DE). H_2 gas was flowed using mass flow controllers (Vögtlin Instruments). Electrochemical control was achieved using an Autolab potentiostat (PGSTAT10) controlled by Gpes software. The three-electrode system used comprised of an isolated Ag/AgCl reference electrode, a graphite rod as a counter electrode and a rotating disk pyrolytic graphite edge plane (PGE) working electrode (area 0.2 cm^2) rotated at 3000 rpm to minimize any mass transport limitations. The whole setup was purchased from Pine Research. All potentials have been converted vs the Standard Hydrogen Electrode (SHE) using the correction E(SHE) = E(Ag/AgCl) + 0.197 at 25°C. Protein films were prepared as follows: the working electrode was abraded using P1000 sandpaper and sonicated in distilled water before being transferred to the anaerobic glovebox (MBRAUN) to equilibrate with the oxygen-free atmosphere. On the following day, a 2 µL drop of 1 - 5 µM enzyme solution was deposited on the electrode surface and let to absorb for 2 - 3 minutes. The excess solution was gently rinsed away with distilled water and the electrode was mounted on the PFE setup to run the experiments. The buffer used was a MES, CHES, HEPES, TAPS and Sodium Acetate (5 mM each) mix with 0.1 M $NaSO_4$ as supporting electrolyte (Mix Buffer). The choice of $NaSO_4$ over the commonly used NaCl was made in order to avoid the occurrence of halides-dependent high-potential inactivation.[9] The buffer was titrated with NaOH or H_2SO_4 to the desired pH. Data was analyzed using Qsoas.[10]

For **1**-HydAB and **2**-HydAB protein film electrochemistry was performed in a similar fashion with the following instrumental differences: The electrochemical cell was contained inside an anaerobic N_2 glovebox (Belle Technologies, O_2 <3 ppm). H_2 gas was flowed using mass flow controllers (Sierra Instruments). Electrochemical control was achieved using an Autolab potentiostat (PGSTAT128N) controlled by Nova software. The PGE working electrode (area 0.03 cm^2) was rotated at a constant speed of 3200 rpm. A Pt wire was used as a counter electrode and a saturated calomel electrode (SCE) was used as a reference. The SCE reference electrode was housed in a separate side arm containing 0.1 M NaCl, which was electrochemically connected to the main cell compartment via a Luggin capillary. Potentials have been converted vs the Standard Hydrogen Electrode (SHE) using the correction E(SHE) = E(SCE) + 0.241 at 25°C.[11] Each protein film was prepared under strict anaerobic condition inside a glovebox (Belle Technologies, O_2 < 3 ppm). First, the PGE electrode was polished with sandpaper (P400, 3M) and thoroughly rinsed with ultrapure water. Then, the enzyme (4 µL of ≈ 6 µM in 10 mm MES pH 5.8 buffer) was applied to the PGE working electrode by pipetting directly onto the electrode surface and leave it to adsorb for 5 min. The unbound protein was removed by rinsing the electrode with ultrapure water before inserting it into the electrochemical cell.

Table S1: Table of FTIR signatures. Table summarizing the FTIR signatures reported for selected redox intermediates of **1**-HydA1 and **1**-HydAB and for the as prepared samples of **2**-HydA1 and **2**-HydAB. Bands assigned to CN stretching modes are underlined.

CrHydA1	**Band positions (cm^{-1})**	**DdHydAB**	**Band positions (cm^{-1})**
2-HydA1, as prep	**2080 1953 1922 1843 1778**	**2**-HydAB, as prep	**2057 1969 1923 1903 1835**
1-HydA1 H_{ox}[12]	2088 2072 1964 1940 1800	**1**-HydAB H_{ox}[13]	2093 2079 1965 1940 1802
1-HydA1 H_{red}[14]	2083 2067 1962 1933 1791	**1**-HydAB H_{red}[15]	2088 2079 1964 1934 1789
1-HydA1 $H_{red}H^{+}$[14, †]	2071 2032 1968 1914 1891	**1**-HydAB $H_{red}H^{+}$[15, †]	2079 2041 1965 1915 1894
1-HydA1 $H_{sred}H^{+}$[16, †]	2070 2026 1954 1919 1882	**1**-HydAB $H_{sred}H^{+}$	*Not reported*

† Data reported from room temperature spectra.

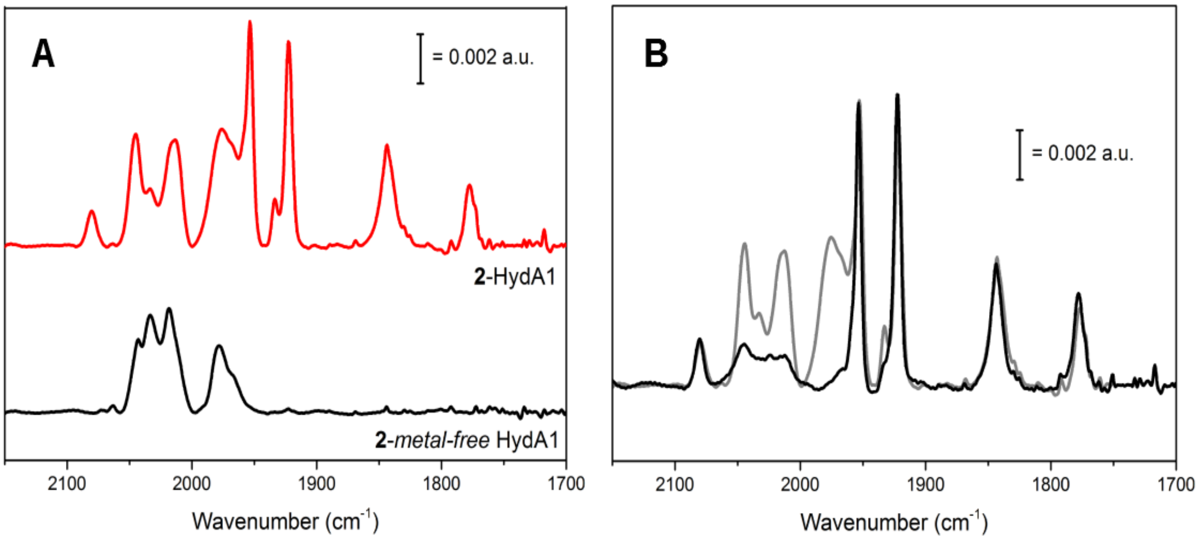

Fig. S1 FTIR spectra of **2**-HydA1 and the effect of light**. Panel A)** ATR-FTIR spectra of an as prepared **2**-HydA1 sample (**red spectrum**). In addition to the sharp H-cluster bands, an additional set of broad peaks can be observed in 2050-1950 cm^{-1} area. These peaks overlap in position with the spectrum of a metal-free HydA1 matured with complex **2** (**black spectrum**). Having been incubated in 20mM NaDT and 10mM EDTA, a metal-free HydA1 lacks the anchoring [4Fe-4S] cluster and is thus unable to form an H-cluster. This leads to the conclusion that these extra peaks belong to non-specifically bound iron species interacting with the protein surface or with the active site pocket. **Panel B)** ATR-FTIR spectra showing the effect of white light illumination on a hydrated **2**-HydA1 film. Upon illumination, the as prepared spectrum **(grey spectrum)** loses the broad components in the 2050-1950 cm^{-1} region while the sharp H-cluster bands remain unchanged. This yields a spectrum with only residual unspecific bands in that region **(black spectrum)**.

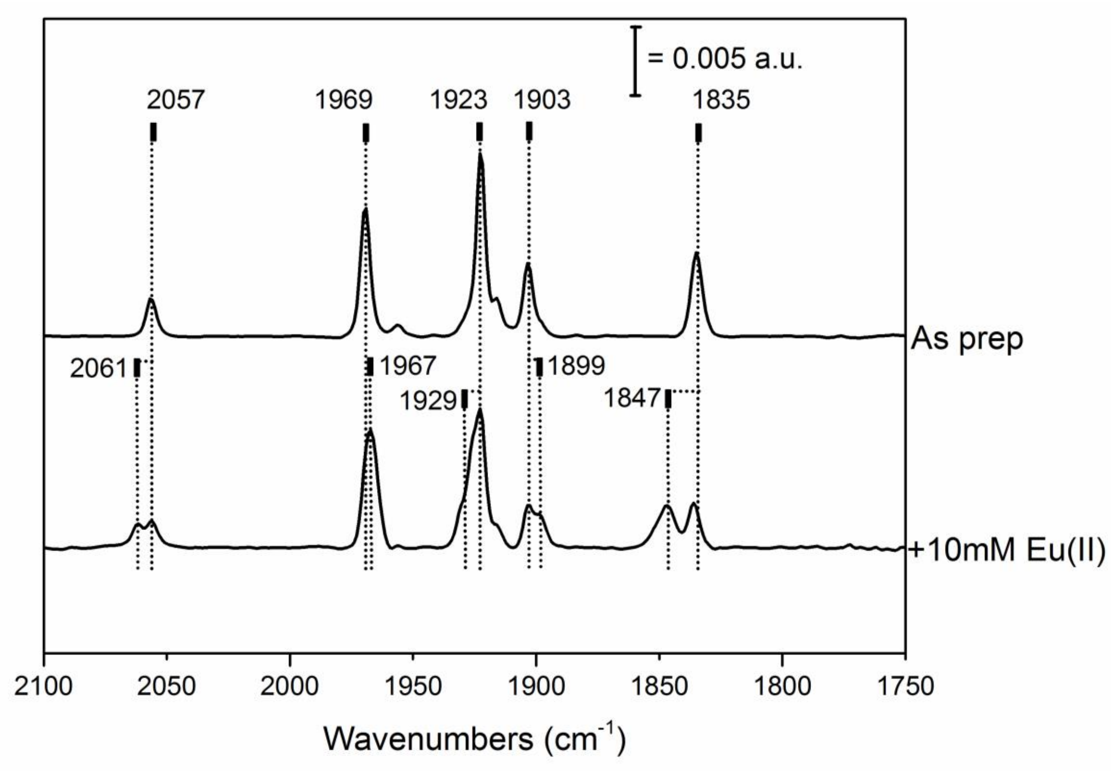

Fig. S2 FTIR spectra showing the effect of Eu(II)-DTPA on 2-HydAB. FTIR spectra are reported for **2**-HydAB 'as prepared' (As prep) and after addition of Eu(II)-DTPA (final concentration 10 mM). The most prominent bands are marked by dotted lines and the corresponding frequencies are indicated on top. Spectra collected at room temperature, on 1.5 mM samples at pH 8, with a 2 cm^{-1} spectral resolution.

It should be noted that a blue-shift of the H_{ox}-state has been observed upon treatment of **1**-HydA1 and **1**-HydAB with NaDT under certain conditions, to yield a state denoted as $H_{ox}H$ or H_{ox}-DT.[7, 17] The exact nature of this state is debated, but as we observe a shift towards higher frequencies also with Eu(II)-DTPA as reductant we can exclude that this is caused by NaDT.

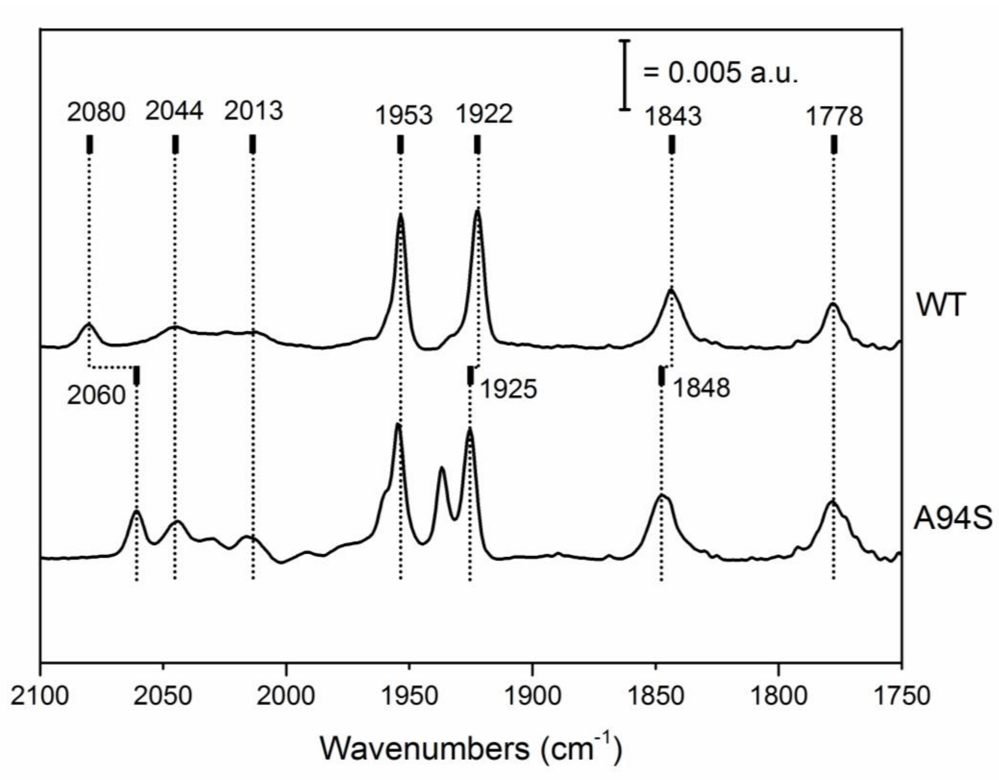

Fig. S3 Effect of the A94S mutation on the FTIR spectrum of **2**-HydA1. Room temperature ATR-FTIR spectra obtained for **2**-HydA1 (WT) and for the A94S mutant. The frequencies of the most prominent bands are given and their shifts can be followed through dotted lines. Spectra are recorded on semi-dry films on an ATR-FTIR crystal, at room temperature and with 2 cm^{-1} spectral resolution.

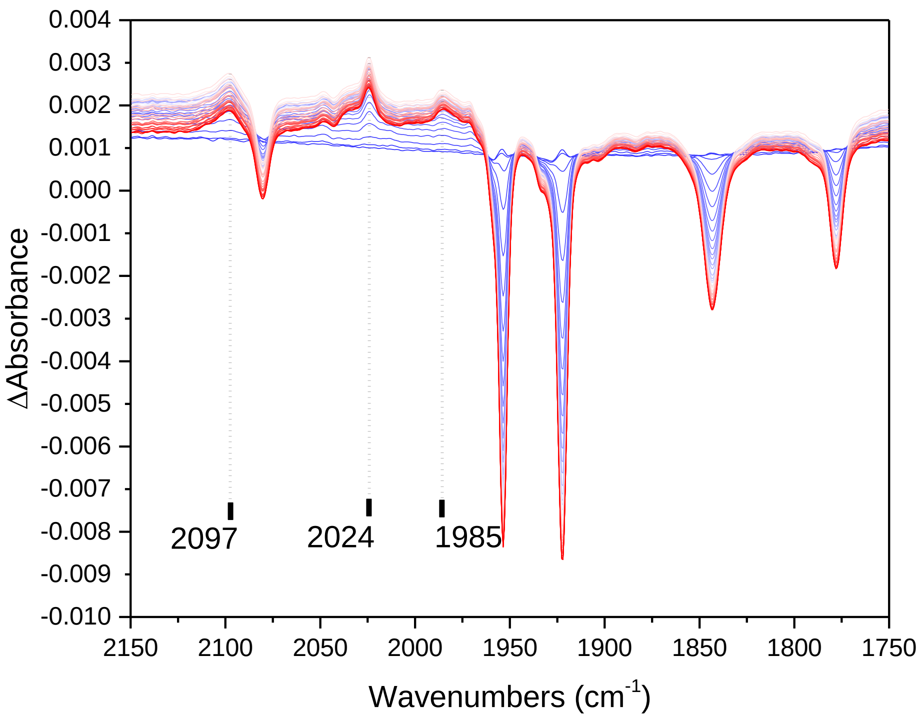

Fig. S4 ATR-FTIR difference spectra of an air-exposed 2-HydA1 semi-hydrated film. Spectra from different time points are overlaid and colored going from **blue to red**, with red spectra being the last to be recorded. The 5 bands attributed to the **2**-HydA1 H-cluster appear as negative peaks, as the cluster itself degrades upon oxygen exposure. Oxygen exposure also triggers the appearance of a set of 3 peaks (2097, 2024 and 1985 cm^{-1}) that, as discussed in the main text, are very close to the mono-iron H_{ox}-air species reported for *Tam*HydS.[18] Notably, no change in the broad light-sensitive bands in the 2050-1950 cm^{-1} region are observed, further indicating that these features belong to non-specifically bound Fe-CO or Fe-CN species that are insensitive to O_2-exposure.

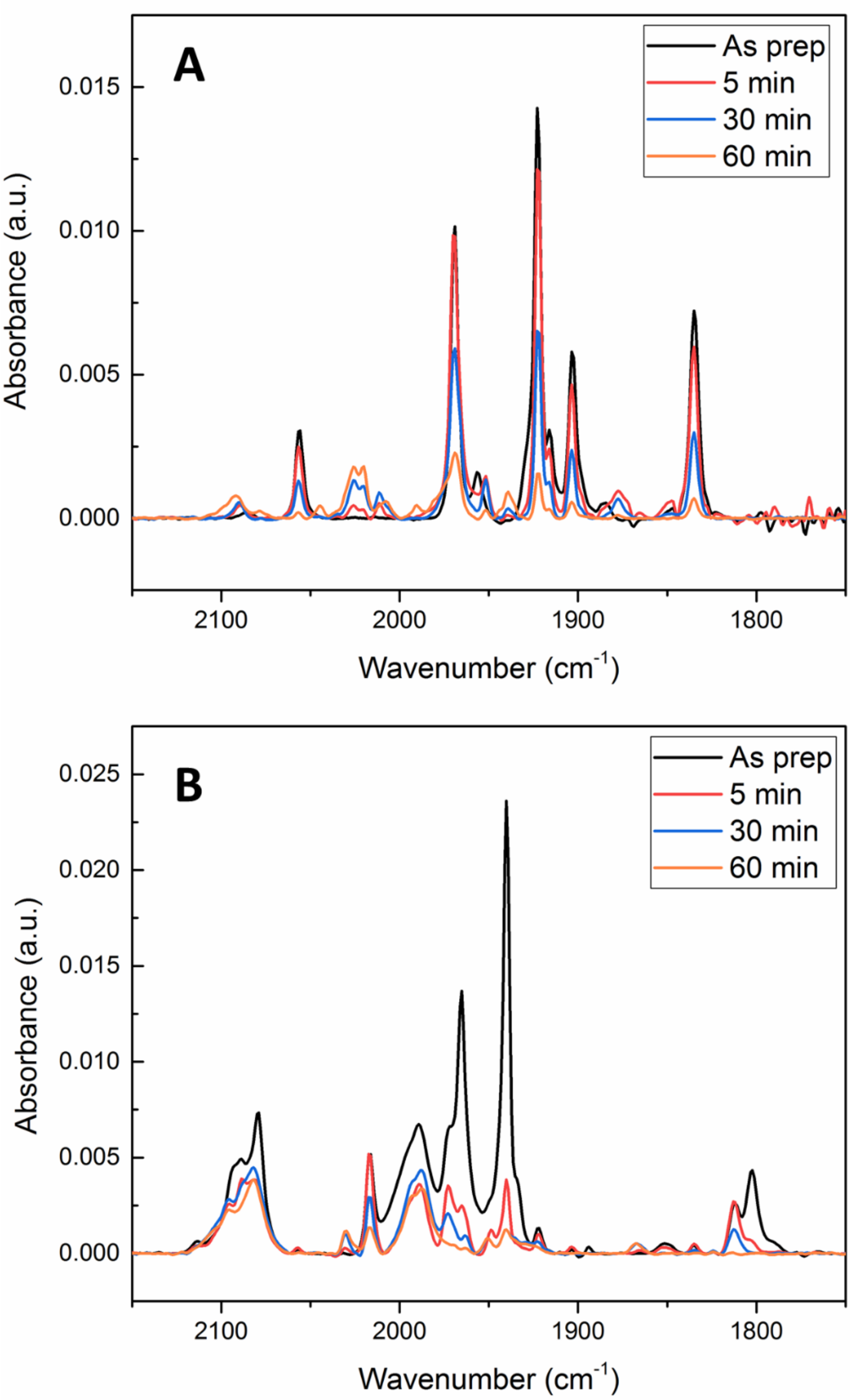

Fig. S5 FTIR spectra showing the effect of O_2 exposure on 1-HydAB and 2-HydAB. Panel A) FTIR spectra showing the effect of O_2 exposure on 2-HydAB. Spectra were recorded before (As prep) and after 5, 30 and 60 minutes of air exposure, and show the degradation of **2**-HydAB's H-cluster signaled by the disappearance of the associated FTIR bands. Panel B) FTIR spectra showing the effect of O_2 exposure on 1-HydAB. Spectra were recorded before (As prep) and after 5, 30 and 60 minutes of air exposure, and show the degradation of **1**-HydAB's H-cluster signaled by the disappearance of the associated FTIR bands. Spectra were collected at room temperature, on 1.07 mM samples at pH 8, with a 2 cm^{-1} spectral resolution.

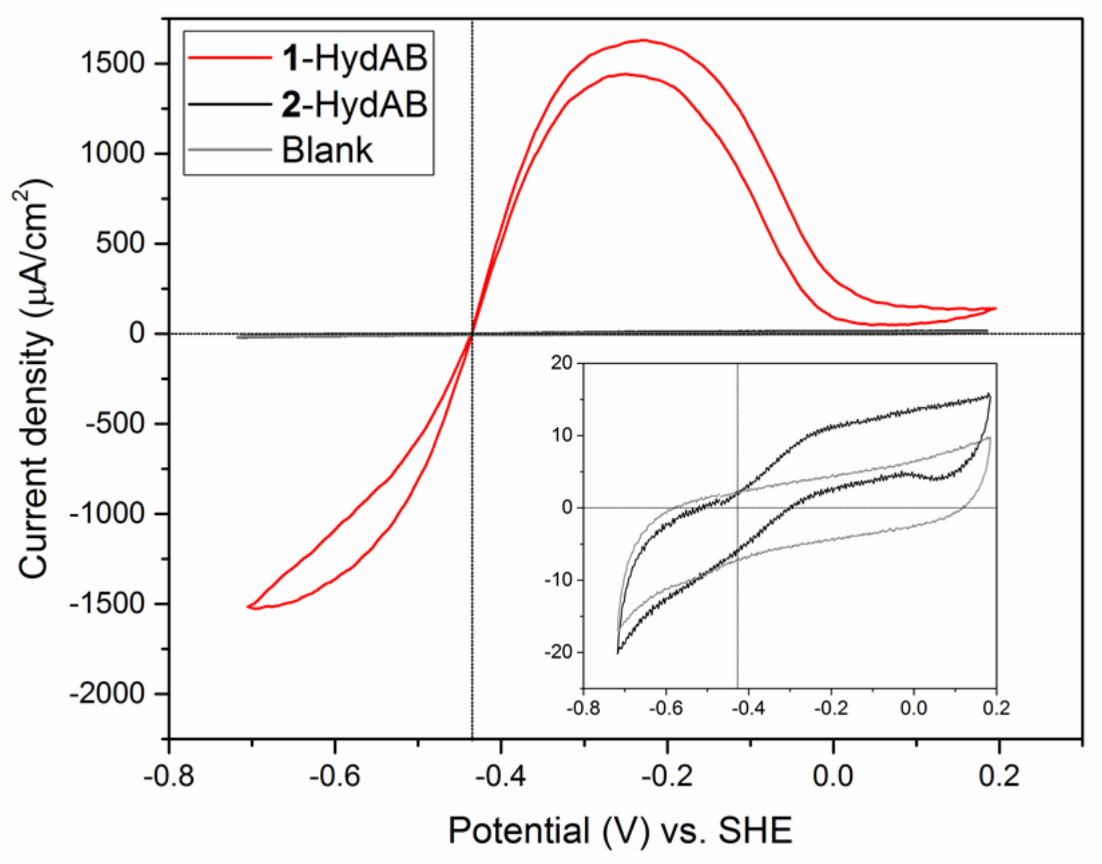

Fig. S6 Cyclic voltammograms of 1-HydAB and 2-HydAB. Cyclic voltammograms of **2**-HydAB (**black trace**) and **1**-HydAB (**red trace**) films absorbed on a rotating-disk PGE electrode, measured in pH 7 Buffer Mix containing NaCl under 1 atm H_2 gas, scan rate: 20 mV/s, temperature: 25°C and rotation rate: 3200 rpm. The **gray trace** represents a blank scan run with the polished electrode (Blank). (**Inset**): A zoom in of the current to highlight a small, but distinctly discernible, contribution from **2**-HydAB. The vertical black dotted-line indicates the thermodynamic potential for the $2H^+/H_2$ couple at pH 7 (E^0= − 0.413 V, vs SHE), while the horizontal black dotted-line represent the zero current.

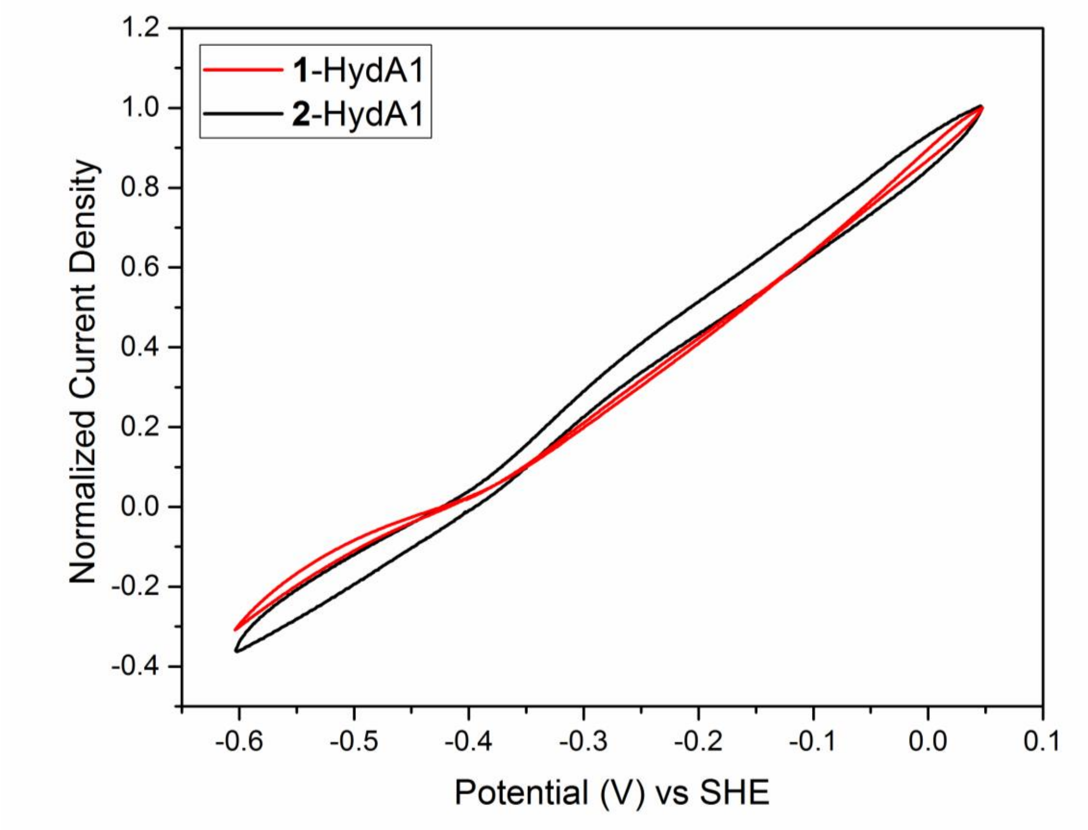

Fig. S7 Cyclic voltammograms with normalized currents for 1-HydA1 and 2-HydA1. Cyclic voltammograms of **2**-HydA1 (black trace) and **1**-HydA1 (red trace) films absorbed on a rotating-disk PGE electrode, measured in pH 7 Buffer Mix under 1 atm H_2 gas, scan rate: 10mV/s, temperature: 30°C and rotation rate: 3000 rpm. Current were normalized at their maximum positive value, at 0.05 mV vs SHE.

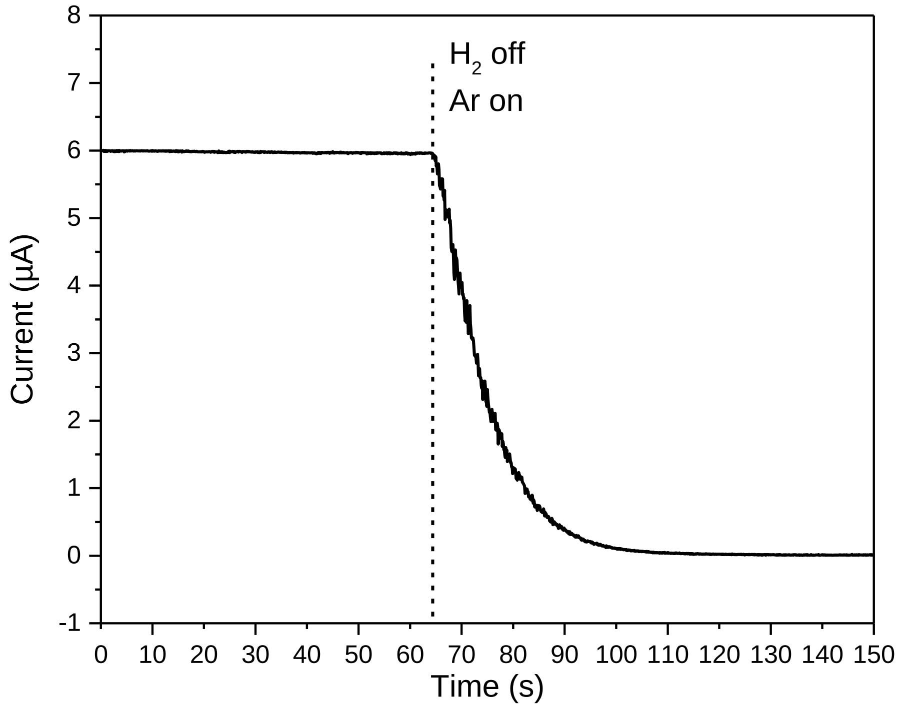

Fig. S8 Determination of K_m through chronoamperometry. Chronoamperometric trace for a **2**-HydA1 protein film on a rotating-disk PGE electrode. Buffer: Mix Buffer pH 7; temperature = 30 °C; electrode potential: − 103 mV vs SHE; electrode area = 0.2 cm^2 and rotation rate: 3000 rpm. The potential was chosen to record H_2 oxidation current vs time. Initial current was recorded under 1 atm of pure H_2 gas. At the switch point indicated on the figure (t = 63 s) H_2 was removed by bubbling 1 atm of argon gas into the electrochemical cell, exponentially decreasing H_2 concentration over time. The current trace was then corrected for film loss. Given the shape of the current decay (not a complete sigmoid), it follows that 1 atm H_2 is not a saturating concentration for the enzyme.[19] Due to technical limitations of the setup, gas pressures above 1 atm could not be reliably probed. Fitting Michaelis-Menten kinetics confirms that **2**-HydA1's K_m for H_2 is ≥ 1 atm.

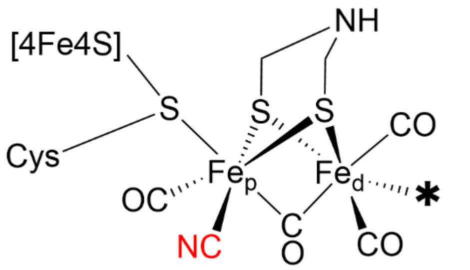

Rotamer I

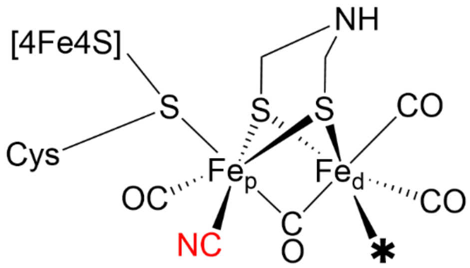

Rotamer II

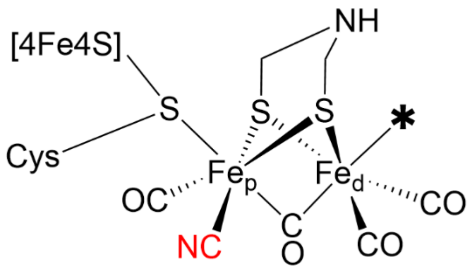

Rotamer III

Fig. S9 Schematic representation of possible rotamers for Fe$_d$ ligands. The three rotamers (I-III) represent possible rotated structures of the H-cluster for the mono-cyanide enzyme variants in the isomer II conformation. An increase in rotational freedom of the Fe$_d$ ligands is hypothesized due to the lack of H-bonding as a result of missing the CN$^-$ ligand in Fe$_d$. The position of the open coordination site is marked with an asterisk as a visual guide. **Rotamer III** represents the expected “functional” conformation, with the open coordination site in an apical position, whereas **Rotamer I** and **Rotamer II** are supposedly non-active alternative conformations.

References

1. C. Esmieu and G. Berggren, *Dalton Trans.*, 2016, **45**, 19242-19248.
2. H. Li and T. B. Rauchfuss, *J. Am. Chem. Soc.*, 2002, **124**, 726-727.
3. L. S. Meszaros, B. Nemeth, C. Esmieu, P. Ceccaldi and G. Berggren, *Angew. Chem. Int. Ed.*, 2018, **57**, 2596-2599.
4. J. A. Birrell, K. Wrede, K. Pawlak, P. Rodriguez-Maciá, O. Rüdiger, E. J. Reijerse and W. Lubitz, *Isr. J. Chem.*, 2016, **56**, 852-863.
5. S. T. Stripp, *ACS Catalysis*, 2021, **11**, 7845-7862.
6. M. Senger, S. Mebs, J. Duan, F. Wittkamp, U.-P. Apfel, J. Heberle, M. Haumann and S. T. Stripp, *Proc. Natl. Acad. Sci. U.S.A.*, 2016, **113**, 8454-8459.
7. M. Senger, S. Mebs, J. Duan, O. Shulenina, K. Laun, L. Kertess, F. Wittkamp, U. P. Apfel, T. Happe, M. Winkler, M. Haumann and S. T. Stripp, *Phys Chem Chem Phys*, 2018, **20**, 3128-3140.
8. S. Stoll and A. Schweiger, *J. Magn. Res.*, 2006, **178**, 42-55.
9. M. del Barrio, M. Sensi, L. Fradale, M. Bruschi, C. Greco, L. de Gioia, L. Bertini, V. Fourmond and C. Léger, *J. Am. Chem. Soc.*, 2018, **140**, 5485-5492.
10. V. Fourmond, *Anal. Chem.*, 2016, **88**, 5050-5052.
11. P. Rodriguez-Maciá, A. Dutta, W. Lubitz, W. J. Shaw and O. Rüdiger, *Angew. Chem. Int. Ed.*, 2015, **54**, 12303-12307.
12. A. Silakov, C. Kamp, E. Reijerse, T. Happe and W. Lubitz, *Biochemistry*, 2009, **48**, 7780-7786.
13. W. Roseboom, A. L. De Lacey, V. M. Fernandez, E. C. Hatchikian and S. P. J. Albracht, *J. Biol. Inorg. Chem.*, 2006, **11**, 102-118.
14. C. Sommer, A. Adamska-Venkatesh, K. Pawlak, J. A. Birrell, O. Rüdiger, E. J. Reijerse and W. Lubitz, *J. Am. Chem. Soc.*, 2017, **139**, 1440-1443.
15. P. Rodríguez-Maciá, K. Pawlak, O. Rüdiger, E. J. Reijerse, W. Lubitz and J. A. Birrell, *J. Am. Chem. Soc.*, 2017, **139**, 15122-15134.
16. A. Adamska, A. Silakov, C. Lambertz, O. Rüdiger, T. Happe, E. Reijerse and W. Lubitz, *Angew. Chem. Int. Ed.*, 2012, **51**, 11458-11462.
17. M. A. Martini, O. Rüdiger, N. Breuer, B. Nöring, S. DeBeer, P. Rodríguez-Maciá and J. A. Birrell, *J. Am. Chem. Soc.*, 2021, **143**, 18159-18171.
18. H. Land, A. Sekretareva, P. Huang, H. J. Redman, B. Németh, N. Polidori, L. S. Mészáros, M. Senger, S. T. Stripp and G. Berggren, *Chem. Sci.*, 2020, **11**, 12789-12801.
19. C. Leger and P. Bertrand, *Chem. Rev.*, 2008, **108**, 2379–2438.